Food and Chemical Toxicology 131 (2019) 110532

Contents lists available at ScienceDirect

Food and Chemical Toxicology

journal homepage: www.elsevier.com/locate/foodchemtox

Determination of genotoxic potencies of pyrrolizidine alkaloids in HepaRG cells using the γH2AX assay

Jochem Louisse[a,*], Deborah Rijkers[a], Geert Stoopen[a], Wendy Jansen Holleboom[a], Mona Delagrange[a], Elise Molthof[a], Patrick P.J. Mulder[a], Ron L.A.P. Hoogenboom[a], Marc Audebert[b], Ad A.C.M. Peijnenburg[a]

[a] RIKILT, Wageningen University and Research, Wageningen, the Netherlands
[b] Toxalim, Research Centre in Food Toxicology, INRA Toulouse, France

ARTICLE INFO

Keywords:
Pyrrolizidine alkaloids (PAs)
HepaRG
Genotoxicity
γH2AX assay
Relative potency factor (RPF)

ABSTRACT

Pyrrolizidine alkaloids (PAs) are secondary metabolites from plants that have been found in substantial amounts in herbal supplements, infusions and teas. Several PAs cause cancer in animal bioassays, mediated via a genotoxic mode of action, but for the majority of the PAs, carcinogenicity data are lacking. It is assumed in the risk assessment that all PAs have the same potency as riddelliine, which is considered to be one of the most potent carcinogenic PAs in rats. This may overestimate the risks, since many PAs are expected to have lower potencies. In this study we determined the concentration-dependent genotoxicity of 37 PAs representing different chemical classes using the γH2AX in cell western assay in HepaRG human liver cells. Based on these *in vitro* data, PAs were grouped into different potency classes. The group with the highest potency consists particularly of open diester PAs and cyclic diester PAs (including riddelliine). The group of the least potent or non-active PAs includes the monoester PAs, non-esterified necine bases, PA *N*-oxides, and the unsaturated PA trachelanthamine. This study reveals differences in *in vitro* genotoxic potencies of PAs, supporting that the assumption that all PAs have a similar potency as riddelliine is rather conservative.

1. Introduction

Pyrrolizidine alkaloids (PAs) are secondary metabolites produced by more than 6,000 plant species, particularly those belonging to the plant families *Asteraceae (Compositae), Boriginaceae* and *Fabaceae (Leguminosae)*, as part of a defense strategy against insects (Hartmann and Witte, 1995; Liu et al., 2017). Several hundreds of PAs have been identified of which 28 have been provisionally selected by the European Commission as relevant in food samples (EFSA, 2016). More recently, the EFSA CONTAM Panel proposed a set of 17 PAs to be monitored in food, but also recommended to include other PAs if possible, in order to better understand the occurrence of PAs in food (EFSA, 2017). Livestock, wildlife and humans are exposed to PAs, which may cause both acute and chronic intoxication (Chen and Huo, 2010; Chojkier, 2003; Fu et al., 2004). Acute toxicity has been reported in developing countries with symptoms of severe intoxication including fatal incidents (Kakar et al., 2010; Robinson et al., 2014). In Europe, risks of PA poisoning in humans are considered to be low, but concerns related to low chronic exposure have increased since the discovery of substantial amounts of PAs in herbal supplements, infusions and teas (Bodi et al., 2014; BfR, 2013; Mulder et al., 2015, 2018). These concerns are felt in view of the reported carcinogenicity of PAs in laboratory animals, mediated via a genotoxic mode of action (Fu et al., 2004; EFSA, 2011; EFSA, 2017). Besides herbal food supplements, herbal infusions and teas, other frequently contaminated human food sources were found to be honey, and to a lesser extent milk and eggs due to the transfer via farm animals (EFSA, 2011, 2016; 2017; BfR, 2013; Mulder et al., 2015, 2018). PAs represent a diverse class of heterocyclic alkaloids that have a pyrrolizidine nucleus (necine base) consisting of two fused, five-membered rings joined by a nitrogen atom, with side chains of various lengths and compositions attached to the 7 and/or 9 position (Fig. 1). PAs can be divided in different categories according to their type of necine base (retronecine (7R), heliotridine (7S), otonecine (7R), and platynecine (7R; saturated)) and their type of esterification (cyclic diesters, open diesters or monoesters) (Fig. 1). Furthermore, the necine base can be oxidized at the nitrogen atom, giving rise to PA *N*-oxides, which are the predominant PA forms in plants (Hartmann and Witte, 1995).

* Corresponding author.
E-mail address: jochem.louisse@wur.nl (J. Louisse).

https://doi.org/10.1016/j.fct.2019.05.040
Received 18 February 2019; Received in revised form 23 May 2019; Accepted 24 May 2019
Available online 30 May 2019
0278-6915/ © 2019 The Authors. Published by Elsevier Ltd. This is an open access article under the CC BY-NC-ND license (http://creativecommons.org/licenses/BY-NC-ND/4.0/).

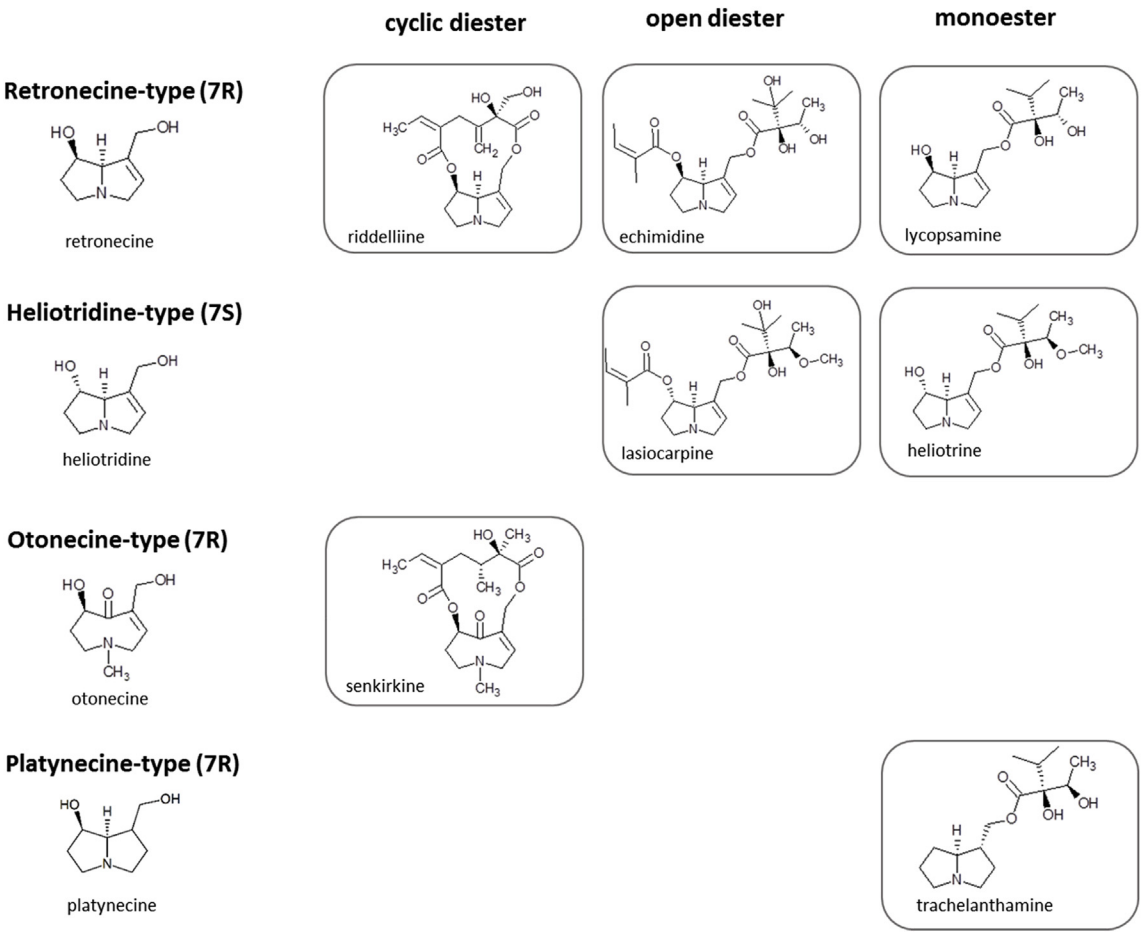

Fig. 1. Overview of various types of PAs exemplified by chemical structures of some of the PAs tested in this study. PAs can be divided in different categories according to their type of necine base (retronecine, heliotridine, otonecine, platynecine) and their type of esterification (cyclic diesters, open diesters or monoesters). The necine base can be oxidized at the nitrogen atom, giving rise to PA N-oxides (not shown).

To exert their toxicity, PAs need to be bioactivated to pyrrolic esters, which are highly reactive molecules that covalently bind with nucleophilic centres in glutathione, proteins or DNA (Ruan et al., 2014a). Bio-activation occurs primarily in the liver by cytochrome P450 (CYP) enzymes, in particular by CYP3A and CYP2B isoforms (Fu et al., 2004), thereby mainly causing hepatotoxicity. Reactions of pyrrolic esters with DNA may lead to DNA damage, ultimately resulting in the formation of tumours, which have been observed in rats upon exposure to lasiocarpine (NTP, 1978), riddelliine (NTP, 2003), monocrotaline (Shumaker et al., 1976), clivorine (Kuhara et al., 1980), senkirkine (Hirono et al., 1979) and symphytine (Hirono et al., 1979). PA *N*-oxides first need to be reduced to their respective PA to enable the formation of the reactive pyrrolic esters (Yang et al., 2017). Platynecine-type PAs (saturated at the 1–2 position) are considered non-toxic, since they cannot be bioactivated to pyrrolic esters (Ruan et al., 2014b).

In the risk assessment of PAs, a precautionary approach is taken, in which it is assumed that all PAs have a similar potency as riddelliine (EFSA CONTAM Panel, 2017). However, this may be too conservative, since, on the basis of available *in vitro* and *in vivo* data, the toxic potency of several PAs has been proposed to be lower than that of riddelliine (Merz and Schrenk, 2016; Chen et al., 2017). For structurally related chemicals with a common mode of action but with different potencies, a relative potency factor (RPF) approach may be used. For each congener of such a group an RPF is determined by expressing its toxic potency relative to the potency of a reference chemical (or index chemical), usually the most potent congener of the group and/or a congener for which adequate toxicity data for the risk assessment are available. Merz and Schrenk (2016) proposed interim RPFs for PAs, based on different *in vitro* data (genotoxicity in *Drosophila* (Wing spot test), cytotoxicity in chicken hepatocellular carcinoma (CLR-2118) cells) and *in vivo* data (LD50 values from acute toxicity studies in rodents upon i.p. or i.v. exposure). From these data, interim RPFs were derived for structurally related subgroups of PAs, amounting to 1.0 for cyclic diesters and heliotridine-type (7S) open diesters (based on data for monocrotaline, retrorsine, riddelliine, senecionine, seneciphylline, senkirkine, heliosupine and lasiocarpine), 0.3 for heliotridine-type (7S) monoesters (based on data for echinatine and heliotrine), 0.1 for retronecine-type (7R) open diesters (based on data for echimidine and symphytine), and 0.01 for retronecine-type (7R) monoesters (based on data for indicine, intermedine and lycopsamine) (Merz and Schrenk, 2016). For the PA *N*-oxides lasiocarpine-*N*-oxide, retrorsine-*N*-oxide and senecionine-*N*-oxide, RPFs were chosen that equal the RPF of the corresponding free base PA, assuming that *N*-oxides completely reduce to their corresponding free base PAs. Although the study of Merz and Schrenk (2016) provides a good starting point to take differences in potencies of PAs into account, the authors indicated that uncertainties prevail about the exact potency of different PA congeners and more (dose-response) data on the toxicity of individual PA congeners are required to establish or refine RPF values for different PA congeners. In that regard, it must be taken into account that species-dependent differences in bioactivation may be expected, indicating that relative potencies obtained from *in vivo* data from laboratory animals may differ from relative potencies in humans.

To obtain more insight in congener-specific differences in toxic potencies of PAs, the present study assessed the concentration-dependent genotoxic responses induced by 37 PAs in human liver HepaRG

cells, using the γH2AX In Cell Western (ICW) assay. This assay detects genotoxic chemicals with diverse DNA damaging properties, including DNA adduct formation, DNA cross-linking and clastogenic effects (Khoury et al., 2013). Histone H2AX plays an important role in the DNA damage response and is phosphorylated into γH2AX upon recognition of DNA double strand breaks (Rogakou et al., 1998). The *in vitro* γH2AX induction data obtained in the present study were used to determine the relative potencies of the tested PAs by performing concentration-response modelling using PROAST benchmark dose (BMD) software. The obtained data provide further insight in congener specific *in vitro* γH2AX induction potencies of PAs, which can be used to refine current interim RPFs for PAs.

2. Materials and methods

2.1. Test chemicals

An overview of the 37 PAs used in the present study and their molecular structures are shown in Supplementary Table 1. Most PAs were purchased from PhytoPlan (Heidelberg, Germany), except for europine, indicine, lasiocarpine, monocrotaline, otosenine, retrorsine *N*-oxide, and trichodesmine, which were obtained from PhytoLab (Vestenbergsgreuth, Germany), trachelanthamine, which was purchased from Latoxan (Portes les valence, France), epi-jacobine, which was obtained from Mercachem (Nijmegen, The Netherlands), usaramine, which was purchased from BOC Sciences (Shirley, NY, USA), and riddelliine, which was a generous gift from Dr. Tao Chen (U.S. FDA). Aflatoxin B1, which was used as a genotoxic reference compound, was obtained from Sigma-Aldrich (Zwijndrecht, The Netherlands). All stock solutions of the compounds and dilutions thereof were prepared in 100% dimethyl sulfoxide (DMSO, Hybri-Max, Sigma-Aldrich).

2.2. HepaRG cell culture

The human hepatic cell line HepaRG was obtained from Biopredic International (Rennes, France) and cultured in growth medium consisting of William's Medium E + GlutaMAX™ (ThemoFisher Scientific, Landsmeer, The Netherlands) supplemented with 10% Good Forte filtrated bovine serum (FBS; PAN™ Biotech, Aidenbach, Germany), 1% PS (100 U/ml penicillin, 100 μg/ml streptomycin; Capricorn Scientific, Ebsdorfergrund, Germany), 50 μM hydrocortisone hemisuccinate (sodium salt) (Sigma-Aldrich), and 5 μg/ml human insulin (PAN™ Biotech). Seeding, trypsinization (using 0.05% Trypsin-EDTA (ThermoFisher Scientific)) and maintenance of the cells was performed according to the HepaRG instruction manual from Biopredic International. For toxicity studies (cell viability and γH2AX induction studies), HepaRG cells were seeded in black-coated 96-well plates (Greiner Bio-One, Frickenhausen, Germany; 9000 cells per well in 100 μL). After two weeks on growth medium, cells were cultured for two days in growth medium supplemented with 0.85% DMSO to induce differentiation. Subsequently, cells were cultured for 12 days in growth medium supplemented with 1.7% DMSO (differentiation medium) for final differentiation. At this stage, cells were ready to be used for toxicity studies. Cells that were not immediately used were kept on differentiation medium for a maximum of three additional weeks. Cell cultures were maintained in an incubator (humidified atmosphere with 5% CO_2 at 37 °C) and the medium was refreshed every 2–3 days during culturing. Prior to toxicity studies, differentiated HepaRG cells were incubated for 24 h in assay medium (growth medium containing 2% FBS) supplemented with 0.5% DMSO.

2.3. Cell exposure

Cells were exposed for 24 h to increasing concentrations of aflatoxin B1 or of one of the PAs. To that end, 200X-concentrated solutions in DMSO were diluted in assay medium, providing a final DMSO concentration of 0.5%. In each experiment a solvent control (0.5% DMSO) and a positive control (aflatoxin B1) was included. Most PAs were tested in concentrations up to 400 μM. After exposure, effects of the test chemicals on cell viability and γH2AX induction were assessed. In each study, each condition was tested in triplicate. Each chemical was tested in three independent studies.

2.4. Cell viability studies

The effect of the chemicals on cell viability was determined using the WST-1 assay. This assay determines the conversion of the tetrazolium salt WST-1 (4-[3-(4-iodophenyl)-2-(4-nitrophenyl)-2H-5-tetrazolio]-1,3-benzene disulfonate) to formazan by metabolically active cells. After exposure for 24 h, the medium was removed and the cells were washed with Dulbecco's Phosphate Buffered Saline (D-PBS; ThermoFisher Scientific). Next, WST-1 solution (Sigma-Aldrich) was added to the cell culture medium (1:10 dilution) and 100 μl was added to each well. After 1 h incubation in an incubator (humidified atmosphere with 5% CO_2 at 37 °C), the plate was shaken at 1000 rpm for 1 min, and absorbance at 450 nm was measured (background absorbance at 630 nm was subtracted) using a microplate reader (Synergy™ HT BioTek, Winooski, VT, USA).

2.5. γH2AX ICW assay

Genotoxic effects of PAs were determined using the γH2AX ICW assay, essentially as previously described (Audebert et al., 2010; Khoury et al., 2013). After exposure for 24 h, the medium was removed and cells were washed with D-PBS. Then cells were fixed with 4% paraformaldehyde (ThermoFisher Scientific) in D-PBS. Subsequently, the cells were washed with D-PBS and incubated for 2 min with a 50 mM NH_4Cl solution (Merck, Darmstadt, Germany). Subsequently, cells were washed with D-PBS, and permeabilized using 0.2% Triton™ X-100 (Sigma-Aldrich) in D-PBS, followed by a washing step with PST solution (0.2% Triton™ X-100 and 2% FBS in D-PBS). After permeabilization, the cells were incubated for 1 h with MAXblock™ Blocking Medium (Active Motif, La Hulpe, Belgium) supplemented with phosphatase inhibitor PhosStop (Sigma-Aldrich) and bovine ribonuclease A (Sigma-Aldrich). This was followed by a 2-h incubation at room temperature with the primary antibody (Phospho-Histone H2A.X (Ser139) (20E3) Rabbit mAb, Cell Signaling Technology, Leiden, The Netherlands) in PST solution. Subsequently, cells were washed three times with PST solution, and incubated with an anti-goat antibody conjugated to an infrared fluorescent dye (Biotium, Fremont, CA, USA) and RedDot™ 2 (for DNA staining, Biotium) in PST solution. The RedDot™ 2 signal is used as a measure for cell number, allowing normalization of the γH2AX-response to cell number. After 1 h of incubation and subsequent three washes with PST solution, plates were scanned using an Odyssey Infrared Imaging System (LiCor ScienceTec, Les Ulis, France; Application Version 3.0). Raw data (integrated intensities, I.I (K counts)) were corrected for the background as described before (Khoury et al., 2013). Subsequently, the γH2AX/DNA fluorescence ratio of each well of the 96-well plate was determined (thereby normalizing for the number of cells), and the fold change for each condition compared to the solvent control was determined by dividing the mean γH2AX/DNA fluorescence ratio by the mean γH2AX/DNA fluorescence ratio of the solvent control. Finally, the mean γH2AX induction and standard deviation of the biological triplicates was determined and the data were subjected to concentration-response modelling. Data were only included when cell viability for that concentration was more than 50% relative to the solvent control. The cell viability limit of 50% was based on the study of Khoury et al. (2013) who applied the γH2AX ICW assay in HepG2 cells. They showed that a cytotoxicity limit of 50% and a γH2AX induction set at ≥ 1.3-fold provides satisfying assay performance (sensitivity, specificity and predictivity) based on a set of model chemicals (Khoury et al., 2013). This cytotoxicity limit of 50% was also

applied for HepaRG cells by Quesnot et al. (2016).

2.6. BMD modelling

Differentiated HepaRG cells were exposed in triplicate (n = 3 technical replicates) in 3 independent experiments (n = 3 biological replicates) for 24 h to increasing concentrations of 37 PA congeners, using the genotoxic and carcinogenic mycotoxin aflatoxin B1 as positive control. For each experiment, the mean of each technical triplicate was obtained. For BMD modelling, three datapoints were used for each concentration of the concentration-response dataset (three means from three independent studies). Concentration-response modelling was solely applied on datasets in which at least one of the concentrations gave rise to ≥1.5-fold γH2AX induction, which has been used as a cut-off for a positive genotoxic response in a previous study in which the γH2AX ICW assay was implemented on HepaRG cells (Quesnot et al., 2016). Concentration-response modelling and benchmark concentration analysis were performed using the PROAST webtool (PROASTweb version 65.2, RIVM, Bilthoven, Netherlands, https://proastweb.rivm.nl), essentially as recommended by EFSA (EFSA Scientific Committee, 2017). PROAST, as well as the US EPA benchmark dose software (BMDS), is particularly applied for modelling of *in vivo* (dose-response) data, providing information on the benchmark dose (BMD). We used the PROAST software for the analysis of *in vitro* (concentration-response) data, thereby providing information on the benchmark concentration (BMC). Tab-delimited text files containing data on concentration, mean γH2AX induction, standard deviation, and sample size (number of biological replicates) were uploaded to the PROAST webtool and analysed as continuous (summary) data. In the tool, data are fitted to a number of mathematical models including three- and four-parameter exponential and Hill models. The two models showing the best (goodness of) fit, i.e. having the lowest Akaike Information Criterion (AIC) value, were used for calculation of the BMC and the corresponding two-sided 90% BMC confidence interval given by the BMCL (lower bound of the BMC confidence interval) and the BMCU (upper bound of the BMC confidence interval). The BMC, BMCL, and BMCU were determined for a benchmark response of 50% (BMR_{50}) which corresponds to a 50% increase over the background level, resulting in a BMC_{50}, $BMCL_{50}$, and $BMCU_{50}$. In PROAST, the used definitions are CES (critical effect size), CED (critical effect dose), CEDL (lower bound of the CED), CEDU (upper bound of the CED), which are identical to BMR, BMC, BMCL, and BMCU, respectively. In order to determine the RPF of a given PA compared to the index PA riddelliine, the ratio of the BMC_{50} of riddelliine and the BMC_{50} of the PA was determined. RPFs below 1 point to a lower potency than riddelliine and RPFs larger than 1 to a higher potency than riddelliine.

3. Results

3.1. Cell viability and γH2AX induction upon treatment of HepaRG cells with PAs

Differentiated HepaRG cells were exposed to increasing concentrations of 37 PA congeners, using the genotoxic and carcinogenic mycotoxin aflatoxin B1 as positive control. For most PAs, concentrations up to 400 μM were used, but for some PAs, 400 μM could not be tested due to poor solubility in the vehicle DMSO (e.g. senecionine). Furthermore, if high cytotoxicity (> 50%) of the PAs was observed in preliminary cell viability experiments (data not shown), these concentrations were not included in the γH2AX induction studies, as explained in the materials and methods.

After exposure, HepaRG cells were subjected to the WST-1 cell viability assay and the γH2AX ICW assay. The results (average and standard deviation of data obtained in the three independent studies) of the γH2AX assay and WST-1 cell viability assay are shown in Fig. 2 and more detailed data are presented in Supplementary Table 2. Although some PAs caused a slight decrease in cell viability at the higher concentrations, induction of γH2AX already appeared at non-cytotoxic concentrations (Fig. 2). A concentration-dependent increase in the induction of γH2AX (resulting in at least 1.5-fold induction at one or more of the concentrations tested) was observed for most of the PAs except for the non-esterified necine bases (heliotridine, otonecine, retronecine), PA *N*-oxides (lasiocarpine *N*-oxide, retrorsine *N*-oxide, senecionine *N*-oxide), the saturated PA trachelanthamine, and the monoesters echinatine, indicine, intermedine, and rinderine. The maximum γH2AX induction by Aflatoxin B1 was slightly higher than 3-fold, which was also observed for the model PAs riddelliine and lasiocarpine, and for several other PAs.

3.2. BMD modelling of γH2AX induction data

The web-based version of PROAST was applied to analyse the concentration-response data and to determine the critical effect concentration, i.e. BMC, corresponding to a 50% increase over the background level (BMC_{50}; 1.5-fold γH2AX induction compared to the background), and associated confidence interval. BMD modelling was only carried out for PAs for which at least at one of the concentrations applied, γH2AX induction was ≥1.5-fold, which was also used as cut-off for genotoxicity in the γH2AX assay performed in HepaRG cells by Quesnot et al. (2016). Using the less stringent cut-off of ≥1.3-fold γH2AX induction as was used by Khoury et al. (2013), would result in the same data inclusion for concentration-response modelling. Since for most PAs that induced γH2AX at least 1.5-fold, the exponential model m5 and Hill model m5 showed the best fit (lowest AIC value), these two models were selected for calculation of the BMC_{50} and the corresponding two-sided 90% BMC confidence interval given by the $BMCL_{50}$ (lower bound of the BMC_{50} confidence interval) and the $BMCU_{50}$ (upper bound of the BMC_{50} confidence interval).

Fig. 3 illustrates the two curves fitted by PROAST for the riddelliine data and shows the BMC_{50}, $BMCL_{50}$ and $BMCU_{50}$ (presented by PROAST as CED, CEDL and CEDU, respectively), being respectively 5.5, 4.3 and 7.2 μM for the exponential model and 5.8, 4.5 and 7.1 for the Hill model. The curves also show that a maximum response is obtained at the highest concentration tested. The results obtained with the Hill and exponential models were very similar. Table 1 provides a summary of the results obtained upon BMD modelling of the concentration-response applying the Hill model. Results obtained when applying the exponential model are presented in the Supplementary Table 3.

3.3. Potency ranking of PAs

To group the PAs based on *in vitro* γH2AX induction potencies, RPFs were determined by calculating the ratio of the BMC_{50} of the index PA riddelliine and the BMC_{50} of the PA of interest upon application of the Hill model (Table 1). RPFs obtained using BMC_{50} values from the exponential model (Supplementary Table 3) were highly similar to those obtained using BMC_{50} values from the Hill model (Table 1). The largest difference in RPF was found for merenskine, amounting to only 1.1-fold. Based on the *in vitro* RPFs, PAs were grouped in four potency groups (Table 1). The group with the highest potency (*in vitro* RPFs between 0.3 and 1.2) consists of 17 PAs for which the BMC_{50} is lower or at maximum three times higher than that of riddelliine, and includes twelve retronecine-type (7R) cyclic diesters (erucifoline, epi-jacobine, integerrimine, jacobine, jaconine, merenskine, merepoxine, retrorsine, riddelliine, senecionine, seneciphylline and senecivernine), two heliotridine-type (7S) open diesters (lasiocarpine and heliosupine) and three retronecine type (7R) open diesters (7-acetylintermedine, 7-acetyllycopsamine and echimidine). The second group (*in vitro* RPFs between 0.1 and 0.3) consists of PAs for which the BMC_{50} is between 3 and 10 times higher than the BMC_{50} of riddelliine and includes two otonecine-type (7S) cyclic diesters (otosenine and senkirkine), and three retronecine-type (7R) cyclic diesters (jacoline, trichodesmine and

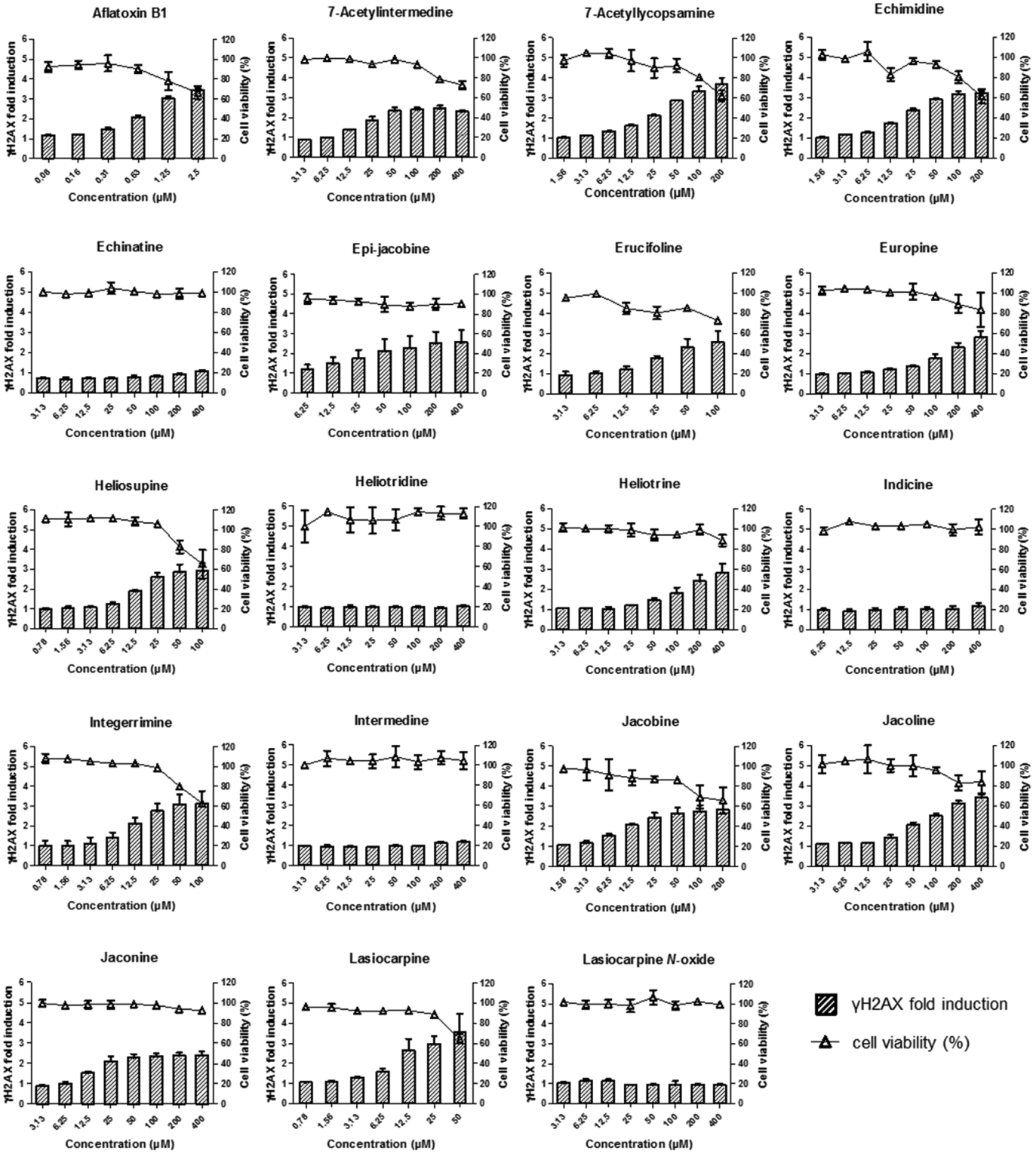

Fig. 2. Concentration-dependent effects of PAs and aflatoxin B1 on HepaRG cell viability (triangles, right Y-axes) and γH2AX induction (bars, left Y-axes). For each condition, mean values (± SD) from three independent experiments are presented.

usaramine). A third group (*in vitro* RPFs between 0.01 and 0.1) consists of four PAs for which the BMC_{50} is between 10 and 100 times higher than the BMC_{50} of riddelliine, including two heliotridine-type (7S) monoesters (europine and heliotrine), the retronecine-type (7R) monoester lycopsamine and the retronecine-type (7R) cyclic diester monocrotaline. The fourth category of least potent PAs (*in vitro* RPFs ≤ 0.01) consists of eleven PAs for which no γH2AX induction was observed or for which γH2AX induction was < 1.5-fold. This fourth category includes the three non-esterified necine bases (retronecine, otonecine, heliotridine), the three PA *N*-oxides (lasiocarpine *N*-oxide, retrorsine *N*-oxide and senecionine *N*-oxide), the platynecine-type PA trachelanthamine, the heliotridine-type (7S) monoesters echinatine and rinderine, and the retronecine-type (7R) monoesters intermedine and indicine. It is of interest to note that the highest concentrations tested of

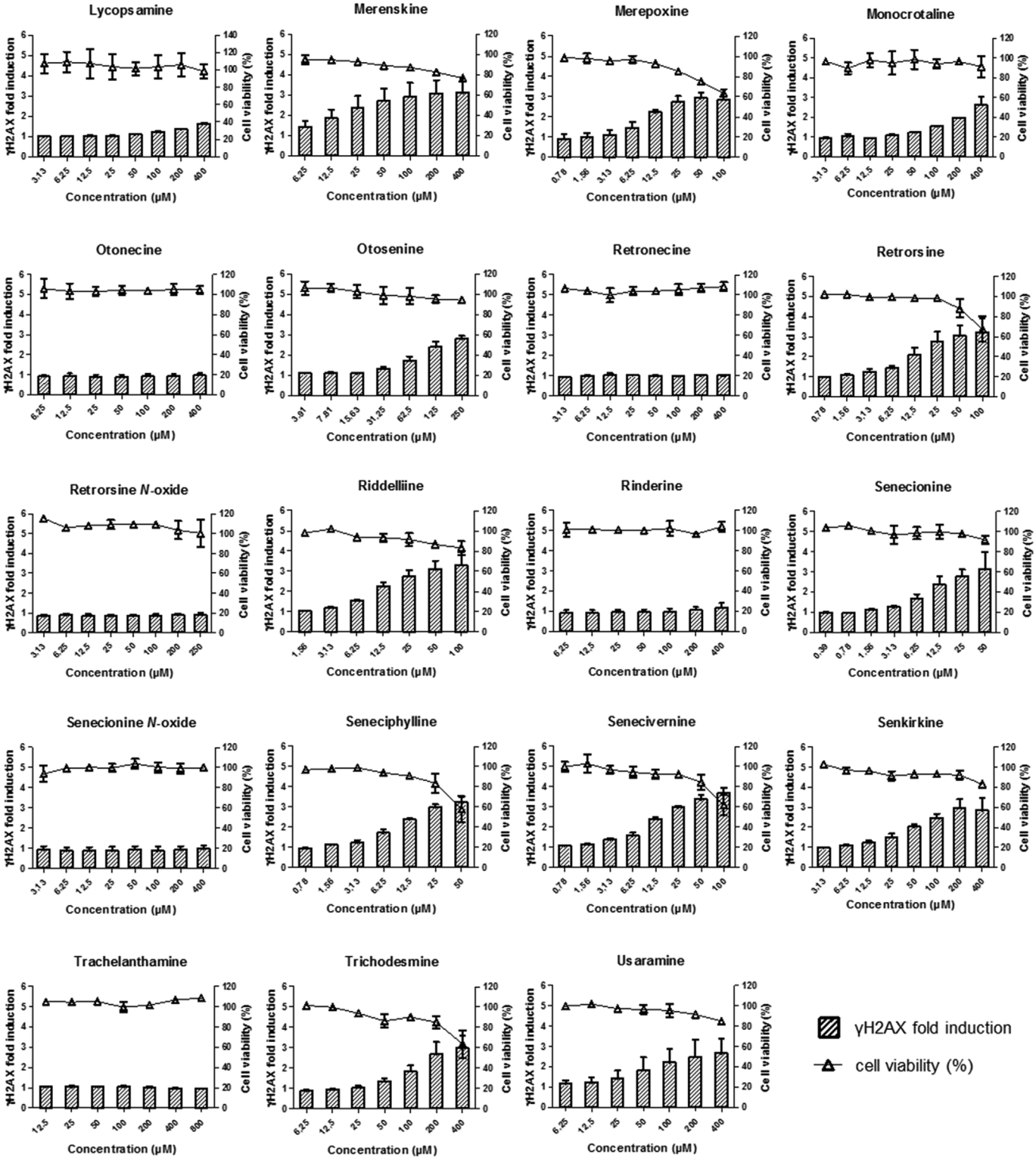

Fig. 2. (*continued*)

these PAs was 400 μM (except for retrorsine *N*-oxide, which was tested at concentrations up to 250 μM and trachelanthamine, which was tested at concentrations up to 800 μM). A PA with a BMC_{50} of 400 μM would provide an RPF of 0.0145 (5.8 μM (= BMC riddelliine)/400 μM). Although these PAs may become active at higher concentrations than 400 μM, it is not likely that the resulting BMC_{50} from those concentration-response datasets would be lower than 400 μM, indicating that the PAs that did not cause a 1.5-fold γH2AX induction at 400 μM are to be placed in group 4, having an RPF ≤ 0.01.

Fig. 4 visualizes the BMC_{50} values including the uncertainties in the estimated BMC_{50}, by presenting the $BMCL_{50}$ and $BMCU_{50}$ of the Hill model for a particular PA as boundaries of the BMC_{50} confidence interval.

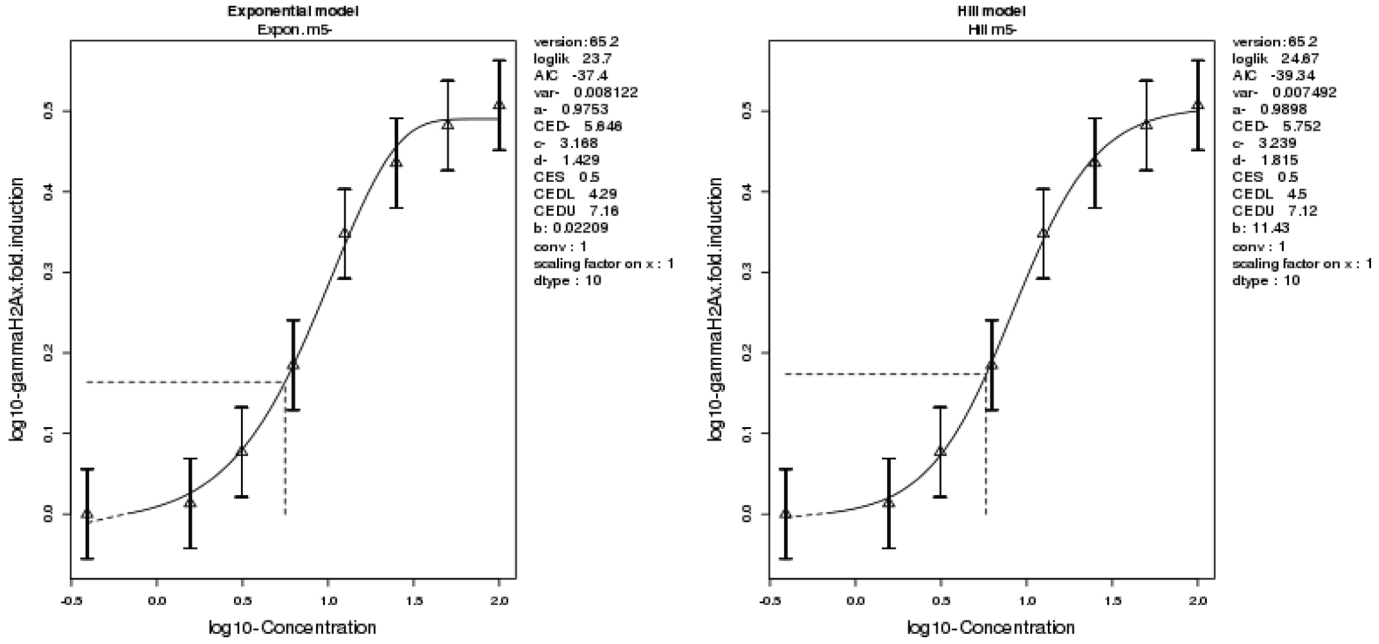

Fig. 3. Results of BMD modelling of concentration-response data (γH2AX induction) for riddelliine. The figure shows the output files generated by PROAST, presenting on the left the best fitted exponential model and on the right the best fitted Hill model. CES: critical effect size (same as BMR), CED: critical effect dose (same as BMC), CEDL: lower bound of the CED (same as BMCL), CEDU: upper bound of the CED (same as BMCU). BMC, BMCL, and BMCU values are calculated for a CES of 0.5, which corresponds to a BMR of 50% (BMR_{50}); the triangles represent average values of three independent experiments; vertical lines (error bars) represent 90% confidence intervals of the average values and the dashed horizontal and vertical lines indicate respectively the BMR of 50% and the corresponding BMD; a,b,c,d represent values for fitted model parameters; for information on other abbreviations, the reader is referred to https://proastweb.rivm.nl.

4. Discussion

The present *in vitro* study determined the concentration-dependent genotoxic effects of a series of PAs using the HepaRG γH2AX ICW assay, with the aim to obtain more insight in relative genotoxic potencies of different PA congeners in human cells. Based on BMD analysis of the concentration-response data, *in vitro* RPFs were derived by calculating the ratio of the BMC_{50} of the index PA riddelliine and the BMC_{50} of each PA. These *in vitro* RPFs, ranging from ≤0.01 to 1.2, were used to group PAs in different potency classes. The data obtained in the present study, together with other data on relative potencies of PAs, may help to refine the interim RPFs of PAs for application in the risk assessment, as proposed by Merz and Schrenk (2016).

Merz and Schrenk (2016) assigned interim RPFs to groups of structurally related PAs based on *in vitro* and *in vivo* data from the literature. In general, the boundaries of the potency classes as defined in the present study are in line with the interim RPFs as proposed by Merz and Schrenk (2016), i.e. potency group 1 (RPF between 0.3 and 1.2) relates to the interim RPF of 1, potency group 2 (RPF between 0.1 and 0.3) relates to the interim RPF of 0.3, potency group 3 (RPF between 0.01 and 0.1) relates to the interim RPF of 0.1, and potency group 4 (RPF ≤ 0.01) relates to the interim RPF of 0.01. Fig. 5 provides insight in how the relative potencies obtained in the present study relate to the interim RPFs as suggested by Merz and Schrenk (2016), excluding the *N*-oxide PAs and the non-toxic platynecine-type (7R) PAs. Merz and Schrenk (2016) assigned an interim RPF of 1 to cyclic diester PAs. Of the cyclic diester PAs tested in the present study, twelve were placed in group 1, five in group 2, and one in group 3. Our data thus indicate that not all cyclic diester PAs should automatically receive an RPF of 1, and that a better understanding of differences in congener-specific potencies of PAs is required. Merz and Schrenk (2016) also assigned an interim RPF of 1 to heliotridine-type (7S) open diester PAs. This is in line with the results of the two heliotridine-type (7S) open diester PAs tested in the present study (heliosupine and lasiocarpine), which were placed in group 1. An interim RPF of 0.3 (group 2) was assigned to heliotridine-type (7S) monoester PAs (Merz and Schrenk, 2016). Of the four PAs of this structural type tested in the present study, two (europine and heliotrine) were placed in group 3 (RPF between 0.01 and 0.1) and two (echinatine and rinderine) were placed in group 4 (RPF ≤0.01). This indicates that an RPF of 0.3 of heliotridine-type (7S) monoester PAs as suggested by Merz and Schrenk (2016) may be too conservative. An interim RPF of 0.1 (group 3) was assigned to retronecine-type (7R) open diester PAs (Merz and Schrenk, 2016). The three PAs of this structural type that were tested in the present study (echimidine, 7-acetylintermedine and 7-acetyllycopsamine) were placed in group 1 (RPF between 0.3 and 1.2), indicating that an RPF of 0.1 of retronecine-type (7R) open diester PAs as suggested by Merz and Schrenk (2016) may not provide sufficient protection when applied in the risk assessment. Finally, Merz and Schrenk (2016) assigned an interim RPF of 0.01 (group 4) to retronecine-type (7R) monoester PAs. We tested three PAs of this type in the present study of which one (lycopsamine) was placed in group 3 (RPF between 0.01 and 0.1) and two (indicine and intermedine) in group 4 (RPF ≤0.01). Of the PAs for which an RPF could be determined in this study, lycopsamine was the least potent, having an RPF of 0.02. This indicates that our results are in line with the proposed interim RPF of 0.01 by Merz and Schrenk (2016) corroborating an RPF of 0.01 for retronecine-type (7R) monoester PAs as proposed by Merz and Schrenk (2016). Summarizing this comparison, our data suggest a higher relative potency of retronecine-type (7R) open diester PAs but a lower relative potency of heliotridine-type (7S) monoester PAs than proposed by Merz and Schrenk (2016). Furthermore, within the structural group of retronecine-type (7R) cyclic diesters, we identified large potency differences, which indicates that application of an RPF of 1 for this structural subgroup may be too conservative for specific PAs. This seems in particular to be the case for monocrotaline.

Several studies reported in the literature have assessed the *in vitro* genotoxic potencies of PAs based on diverse genotoxicity assays (see review by Chen et al., 2010). Potency rankings have been reported for the PA-induced DNA cross-linking formation in bovine kidney epithelial cells (Hincks et al., 1991) and PA-induced genotoxicity in the wing spot

Table 1
Overview of BMC_{50}, $BMCL_{50}$ and $BMCU_{50}$ values determined upon BMD modelling (applying the Hill model) of data on γH2AX induction by the PAs tested in the present study. Also presented are the RPF values, which are derived by dividing the BMC of riddelliine by the BMC of the respective PA. These RPF values were used for grouping the PAs in four potency groups (group 1: RPF 0.3–1.2, group 2: RPF 0.1–0.3, group 3: RPF 0.01–0.1, group 4: RPF ≤0.01). Interim RPFs as suggested by Merz and Schrenk (2016) are given in the last column. Interim RPFs of PAs given in brackets are of PAs that were not included in the study of Merz and Schrenk (2016), but belong to the respective structural groups identified by Merz and Schrenk (2016), amounting to 1.0 for cyclic diester and heliotridine-type (7S) open diester PAs, 0.3 for heliotridine-type (7S) monoester PAs, 0.1 for retronecine-type (7R) open diester PAs, and 0.01 for retronecine-type (7R) monoester PAs.

Chemical	necine base	esterification	BMC	BMCL	BMCU	RPF	*in vitro* potency	Interim RPF[a]
			(μM)					
Aflatoxin B1	NA	NA	0.48	0.43	0.52	12	NA	NA
Senecionine	Re (7R)	cyclic diester	4.6	3.4	5.9	1.24	group 1	1
Seneciphylline	Re (7R)	cyclic diester	4.8	4.0	5.6	1.20	group 1	1
Senecivernine	Re (7R)	cyclic diester	5.1	4.2	6.1	1.13	group 1	[1]
Lasiocarpine	He (7S)	open diester	5.3	3.8	6.9	1.08	group 1	1
Riddelliine	Re (7R)	cyclic diester	5.8	4.5	7.1	1.00	group 1	1
Jacobine	Re (7R)	cyclic diester	6.1	4.9	7.4	0.94	group 1	[1]
Merenskine	Re (7R)	cyclic diester	6.2	4.6	8.1	0.92	group 1	[1]
Retrorsine	Re (7R)	cyclic diester	6.4	4.4	8.5	0.90	group 1	1
Integerrimine	Re (7R)	cyclic diester	7.6	5.3	10	0.75	group 1	[1]
Jaconine	Re (7R)	cyclic diester	7.7	6.7	8.7	0.75	group 1	[1]
7-Acetylintermedine	Re (7R)	open diester	8.8	7.4	10	0.65	group 1	[0.1]
Heliosupine	He (7S)	open diester	8.8	7.5	10	0.65	group 1	1
Merepoxine	Re (7R)	cyclic diester	8.8	4.8	8.7	0.65	group 1	[1]
Echimidine	Re (7R)	open diester	9.4	8.3	11	0.61	group 1	0.1
7-Acetyllycopsamine	Re (7R)	open diester	10	8.6	11	0.58	group 1	[0.1]
Epi-jacobine	Re (7R)	cyclic diester	12	7.7	18	0.48	group 1	[1]
Erucifoline	Re (7R)	cyclic diester	17	13	22	0.33	group 1	[1]
Senkirkine	Ot (7R)	cyclic diester	25	18	32	0.23	group 2	1
Usaramine	Re (7R)	cyclic diester	28	15	46	0.20	group 2	[1]
Jacoline	Re (7R)	cyclic diester	30	26	35	0.19	group 2	[1]
Otosenine	Ot (7R)	cyclic diester	51	42	59	0.11	group 2	[1]
Trichodesmine	Re (7R)	cyclic diester	58	43	73	0.10	group 2	[1]
Heliotrine	He (7S)	monoester	62	45	80	0.09	group 3	0.3
Europine	He (7S)	monoester	62	49	75	0.09	group 3	[0.3]
Monocrotaline	Re (7R)	cyclic diester	89	73	107	0.06	group 3	1
Lycopsamine	Re (7R)	monoester	303	269	342	0.02	group 3	0.01
Echinatine	He (7S)	monoester	NA	NA	NA	≤0.01	group 4	0.3
Rinderine	He (7S)	monoester	NA	NA	NA	≤0.01	group 4	[0.3]
Intermedine	Re (7R)	monoester	NA	NA	NA	≤0.01	group 4	0.01
Indicine	Re (7R)	monoester	NA	NA	NA	≤0.01	group 4	0.01
Otonecine	Ot (7R)	none	NA	NA	NA	≤0.01	group 4	NA
Heliotridine	He (7S)	none	NA	NA	NA	≤0.01	group 4	NA
Retronecine	Re (7R)	none	NA	NA	NA	≤0.01	group 4	NA
Lasiocarpine *N*-oxide	He (7S)	open diester	NA	NA	NA	≤0.01	group 4	1[b]
Retrorsine *N*-oxide	Re (7R)	cyclic diester	NA	NA	NA	≤0.01	group 4	1[b]
Senecionine *N*-oxide	Re (7R)	cyclic diester	NA	NA	NA	≤0.01	group 4	1[b]
Trachelanthamine	Pl	monoester	NA	NA	NA	≤0.01	group 4	NA

NA: not applicable.
[a] Interim RPF as suggested by Merz and Schrenk (2016).
[b] For PA N-oxides, Merz and Schrenk (2016) suggested the same potency as the corresponding free base PAs, assuming that N-oxides are completely reduced to their corresponding free base PAs.

test of *D. melanogaster* (Frei et al., 1992). Genotoxicity data from the wing spot test of *D. melanogaster* were used by Merz and Schrenk (2016) for the derivation of interim RPFs. The data obtained in the present study are most in line with the ranking obtained by Hincks et al. (1991), whereas more discrepancies are observed with the ranking obtained by Frei et al. (1992). Differences in relative potencies may be related to differences in both metabolic activation in the *in vitro* models and differences in genotoxicity readouts. Regarding metabolic activation, the human HepaRG model used in the present study is considered to be relevant, expecting to represent both relevant human bioactivation and detoxification activities. Regarding the genotoxicity readout, we consider phosphorylation of histone H2AX (γH2AX) to be a relevant readout for determining *in vitro* relative genotoxic potencies of PAs, since PAs have been reported to have divergent DNA damaging properties (PA-induced adduct formation, DNA cross-linking and clastogenic effects (Chen et al., 2010)) and since the γH2AX ICW assay has been reported to detect genotoxins with such DNA damaging properties (Khoury et al., 2013). On the other hand, one must consider that chemical-induced apoptosis may induce γH2AX (Lu et al., 2006; Wu et al., 2015). In our study, γH2AX induction was already observed at concentrations far below cytotoxic concentrations, indicating that γH2AX was not induced because of PA-induced apoptosis. With increasing PA concentrations, cells will eventually go into apoptosis when DNA damage is such that it cannot be repaired (Norbury and Zhivotovsky, 2004; Roos and Kaina, 2006; Wang, 2001). Nikolova et al. (2014) found a correlation between cytotoxicity and γH2AX induction for genotoxic agents, whereas for nongenotoxic agents, cytotoxicity was not related to γH2AX induction. Taking this latter study into account and given that in our studies γH2AX induction was already observed at concentrations far below cytotoxic concentrations, we are confident that we have measured γH2AX induction related to DNA damaging effects induced by the PAs. Eleven of the PAs tested in the present study did not induce γH2AX ≥ 1.5-fold up to the highest concentration tested. These PAs were grouped in the lowest potency group (group 4: RPF < 0.01). This group includes the platynecine-type PA trachelanthamine, which has been reported to be not genotoxic since the necine base of this PA type is saturated and can therefore not be bioactivated to toxic pyrrolic esters (Ruan et al., 2014b). It also contains

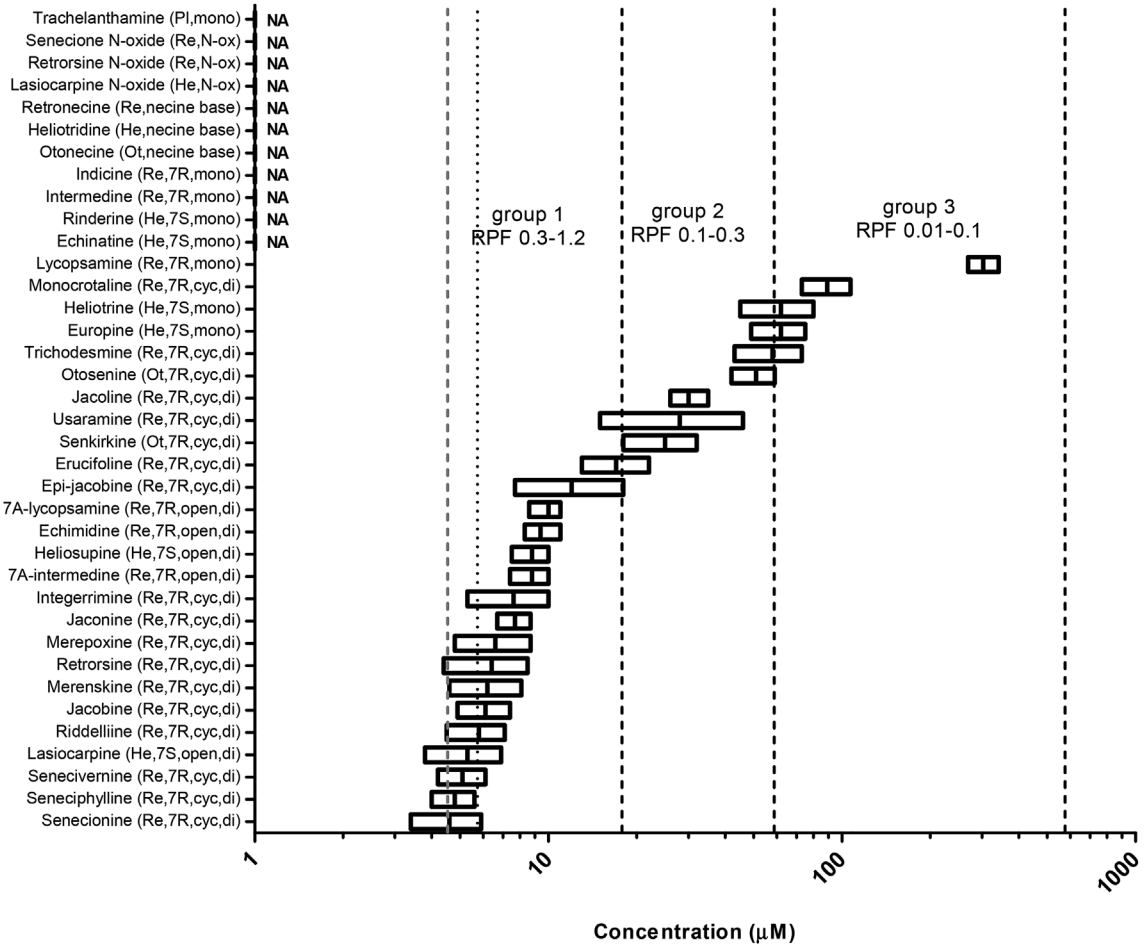

Fig. 4. Range between $BMCL_{50}$ and $BMCU_{50}$ values of PA-mediated γH2AX induction obtained by the Hill model. The BMC_{50} values, presented by the vertical stripe in the bars, have been used for determination of RPF values for individual PAs (Table 1). Vertical dashed lines provide the boundaries between the *in vitro* potency groups, being group 1: PAs with RPFs between 0.3 and 1.2, group 2: PAs with RPFs between 0.1 and 0.3, and group 3: PAs with RPFs between 0.01 and 0.1. The vertical dotted line represents the BMC of the index PA riddelliine, having by definition an RPF of 1. Group 4 contains the PAs that were not active (NA; not able to induce γH2AX ≥1.5-fold up to 400 µM) having an RPF ≤ 0.01.

the non-esterified necine bases retronecine, heliotridine and otonecine, which are also expected to be negative. This group includes also the retonecine-type (7R) monoesters indicine and intermedine and the heliotrine-type (7S) monoesters echinatine and rinderine. It should be noted that these PAs showed some minor effects, but not sufficient to reach a 1.5-fold induction at the highest concentration included in this study. Furthermore, the three PA *N*-oxides tested in the present study were negative.

Recently, Allemang et al. (2018) determined the concentration-dependent PA-induced formation of micronuclei in HepaRG cells by exposing the cells to 15 PAs representing the same six structural classes as tested in this study (retronecine-type (7R) cyclic diesters, heliotridine-type (7S) open diesters, retronecine-type (7R) open diesters, retronecine-type (7R) monoesters, heliotridine-type (7S) monoesters, and platynecine-type (7R) cyclic diesters). Of these 15 PAs, eleven were also tested in the present study. In general, some similarities and discrepancies in relative potencies of the PAs that were tested positive in both studies can be identified. In both studies lasiocarpine, riddelliine, retrorsine and echimidine have a relatively high potency, and indicine, intermedine, lasiocarpine *N*-oxide, lycopsamine, monocrotaline, and europine a relatively low potency. The main discrepancy between the two *in vitro* studies was found for heliotrine, which was relatively potent in the micronucleus assay, but not in the γH2AX ICW assay. Furthermore, in the micronucleus assay, lasiocarpine was by far the most potent PA (e.g. 6 and 10 times more potent than riddelliine and retrorsine, respectively), whereas in the γH2AX ICW assay, lasiocarpine had a similar potency as riddelliine and retrorsine. Lasiocarpine *N*-oxide was negative in the present study and positive in the micronucleus assay, albeit only at high concentrations (BMC_{50} values > 400 µM). Indicine and intermedine, which were positive in the micronucleus assay, showed a slight induction of γH2AX, but these were lower than 1.5-fold, and therefore not used for concentration-response analysis. Differences in genotoxic responses obtained between the present study and that of Allemang et al. (2018) may be related to differences in the readout for genotoxicity, in vehicle used (DMSO was used for all PAs in the present study, water for most PAs in the study of Allemang et al. (2018)), and/or differences in study set-up. Regarding the latter, in both assays HepaRG cells are used and an exposure duration of 24 h is applied. However, cells are immediately fixed after exposure and analysed for γH2AX induction in the γH2AX ICW assay, whereas in the HepaRG micronucleus assay, cells were incubated for three days with human epidermal growth factor after the 24-h PA exposure, to induce cell proliferation allowing micronuclei formation (Allemang et al., 2018). Furthermore, Allemang applied concentrations up to 1000 µM, whereas the highest concentration applied in the present study was 400 µM. It is of interest to note that the platynecine-type (7R) PA platyphylline, which was not tested in the present study, was slightly positive (BMC_{50} > 200 µM) in the HepaRG micronucleus assay (Allemang et al., 2018), whereas one would expect it to be negative because of the saturated platynecine base, which cannot be

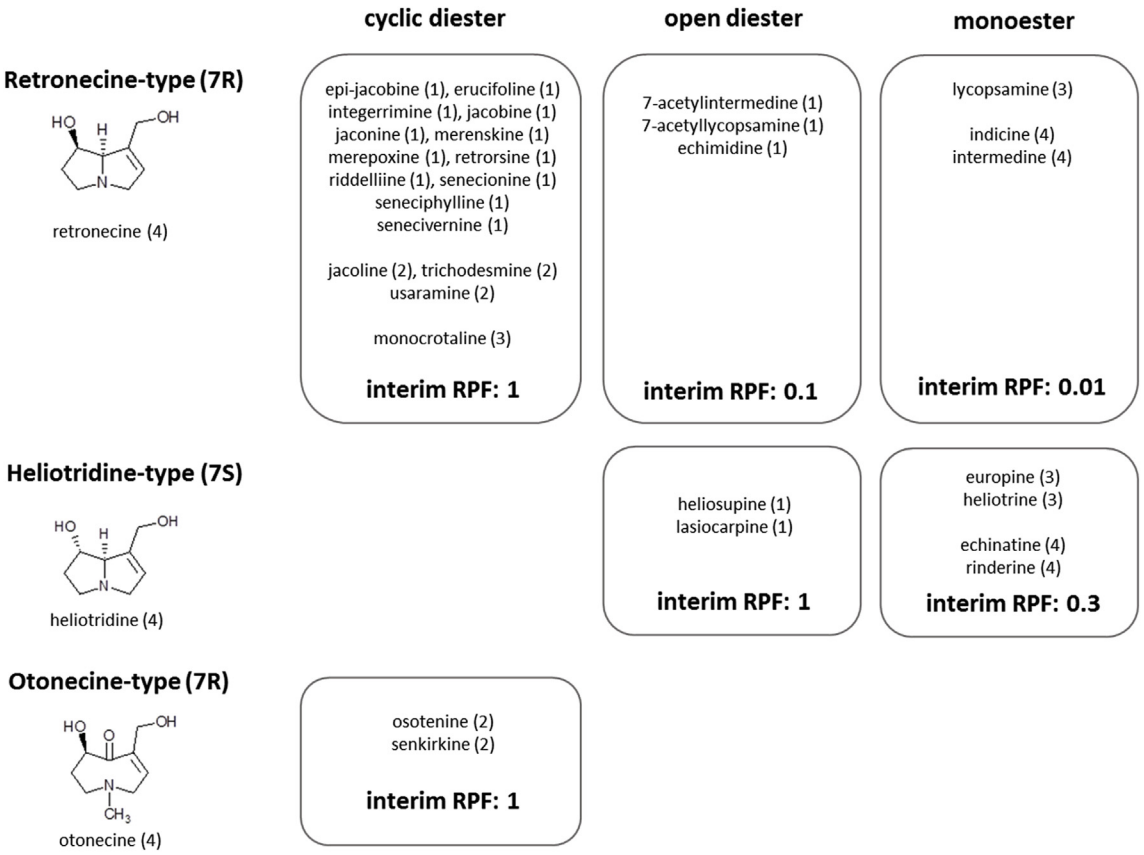

Fig. 5. Overview of potencies of PAs tested in present study in relation to the interim RPFs as suggested by Merz and Schrenk (2016) for structurally related subgroups of PAs. Merz and Schrenk (2016) derived an interim RPF of 1.0 for cyclic diester and heliotridine-type (7S) open diester PAs, an interim RPF of 0.3 for the heliotridine-type (7S) monoester PAs, an interim RPF of 0.1 for retronecine-type (7R) open diester PAs, and an interim RPF of 0.01 for retronecine-type (7R) monoester PAs. PAs tested in the present study are presented according to the structural subgroup they belong to and the *in vitro* potency group as determined in the present study is given in brackets (group 1: RPF 0.3–1.2; group 2: RPF 0.1–0.3; group 3: RPF 0.01–0.1; group 4: RPF ≤ 0.01).

bioactivated to a pyrrolic ester (Ruan et al., 2014b).

All PA *N*-oxides tested in the present study were negative, whereas Allemang et al. (2018) tested PA *N*-oxides positive, albeit only at high concentrations (BMC_{50} values > 400 μM). Studies with rat and human liver microsomes have indicated that PA *N*-oxides are reduced by liver fractions to the free base PAs, but the enzymes responsible for such reactions have not been elucidated (Wang et al., 2005; Yang et al., 2017). From our study we cannot conclude whether HepaRG cells are able to reduce PA *N*-oxides, but our results indicate that possible PA *N*-oxide reduction to the free base PAs was not efficient enough to obtain sufficient free base PAs that cause γH2AX induction within the total exposure time frame of 24 h. Another reason for a negative response for PA *N*-oxides may be a possible lower uptake of PA *N*-oxides than the free base PAs in the HepaRG cells. The negative response of PA *N*-oxides in the present study also indicates that the PA *N*-oxide standards used in the present study were free of (or very low in) traces of the free bases. Indeed, a 1% of free base present in 400 μM lasiocarpine *N*-oxide or senecionine *N*-oxide would provide a positive response in the γH2AX assay. Merz and Schrenk did not derive specific RPFs for *N*-oxides, but suggested to use RPFs that equal the RPF value of the corresponding free PA, assuming that *N*-oxides are completely reduced. An *in vivo* study in rats that were exposed to either senecionine or senecionine *N*-oxide showed large differences in kinetics, resulting in remarkable differences in internal concentrations of both senecionine and senecionine *N*-oxide (Yang et al., 2017). Another *in vivo* study, in which rats were exposed to retrorsine, riddelliine, monocrotaline or their *N*-oxides, showed that DNA adduct levels in the liver were 3–10 times higher upon exposure to the free base PAs compared to the PA *N*-oxides (Yang et al., 2017), indicating that the interim RPFs for *N*-oxides as proposed by Merz and Schrenk (2016) may be too conservative.

In order to use RPFs obtained from *in vitro* studies for the risk assessment, they should be in line with relative potencies of PAs *in vivo*. Chen et al. (2017) assessed available rodent carcinogenicity data and estimated relative potencies for five PAs compared to lasiocarpine. Of these five PAs, three were tested in the present study, of which riddelliine is correctly predicted to have a similar potency as lasiocarpine. Furthermore, senkirkine and monocrotaline are correctly predicted to have a lower potency. Although this *in vitro-in vivo* comparison is of help to evaluate to RPFs obtained *in vitro*, it should be taken into account that the available *in vivo* carcinogenicity data are limited and that the available data for senkirkine and monocrotaline were not suitable to perform an adequate dose-response analysis (Chen et al., 2017), indicating that relative potencies obtained with these data should be used with care. Furthermore it should be taken into account that species-dependent differences in PA bioactivation may result in differences in relative potencies in humans compared to those in laboratory animals. The *in vitro* RPFs derived in the present study are based on (nominal) effect concentrations at target cells, whereas the concentrations that will be present at the target cells in the *in vivo* situation depend on *in vivo* kinetic processes (absorption, distribution, metabolism and excretion (ADME)), which may differ between one PA congener to the other, and which may differ for the same PA between different species. An *in vitro* transport study using Caco-2 and MDCKII/ABCB1 cells showed that differences in *in vivo* intestinal translocation can be expected between different PA congeners (Hessel et al., 2014). That study showed that intestinal translocation of heliotrine and especially echimidine is expected to be lower compared to that of senkirkine and senecionine because of active P-glycoprotein-mediated transport of PAs from

intestinal cells back to the gut lumen. Furthermore, differences in *in vivo* metabolism between different PA congeners may be expected, since congener-specific differences in PA depletion and pyrrolic ester formation, as measured in *in vitro* incubations with liver fractions, have been reported (Ruan et al., 2014a; Kolrep et al., 2018). To further refine RPFs of PAs based on *in vitro* relative potency data, information on relative availability of PA congeners at the target site is required (e.g. concentration reached in the liver of a particular PA at a certain oral dose, relative to the concentration reached in the liver of the index PA (riddelliine) at the same oral dose). This may be achieved by applying physiologically based kinetic (PBK) modelling, which integrates all information related to ADME processes and allows the dose-dependent estimation of internal concentrations at the target site. As such, RPFs can be derived by multiplying the *in vitro* RPF by the PBK model-predicted relative availability *in vivo*. Recently, Chen et al. (2018) and Ning et al. (2019) used a PBK modelling-based reverse dosimetry approach for lasiocarpine and riddelliine for rats and humans, respectively, aiming to translate *in vitro* hepatoxicity (cytotoxicity) data to predicted *in vivo* dose levels that cause hepatoxicity. When more of such *in silico* models (for other PAs) become available, insight in PA congener-specific relative internal concentrations can be obtained, which can be applied to estimate *in vivo* RPFs based on *in vitro* RPFs. However, one must realize that even when (differences in) kinetics are taken into account, uncertainties remain in how *in vitro* genotoxic potencies relate to *in vivo* carcinogenicity potencies, which is an issue that requires further investigation before these *in vitro* derived RPFs can be applied in the risk assessment.

Altogether, the present study provides data on the relative *in vitro* genotoxic potencies of a large series of PAs of diverse structural subclasses, showing differences spanning several orders of magnitude. The data obtained in the present study, together with other data on relative genotoxicity potencies of PAs, e.g. as obtained with the micronucleus assay (Allemang et al., 2018), may help to refine the interim RPFs of PAs for application in the risk assessment, as proposed by Merz and Schrenk (2016). Further work on toxicokinetic parameters is needed allowing the translation of *in vitro* RPFs to *in vivo* RPFs and application of the refined RPFs for the risk assessment of PAs. The present work supports previous studies showing that the assumption that all PAs have a similar potency as riddelliine is rather conservative.

Acknowledgements

This work was supported by the Dutch Ministry of Economic Affairs (project WOT-02-002-003).

Appendix A. Supplementary data

Supplementary data to this article can be found online at https://doi.org/10.1016/j.fct.2019.05.040.

Transparency document

Transparency document related to this article can be found online at https://doi.org/10.1016/j.fct.2019.05.040.

References

Bundesinstitut für Risikobewertung (BfR), 2013. Pyrrolizidine alkaloids in herbal teas and teas. BfR Opin. 2013 No. 018/2013 of 5 July.
Allemang, A., Mahony, C., Lester, C., Pfuhler, S., 2018. Relative potency of fifteen pyrrolizidine alkaloids to induce DNA damage as measured by micronucleus induction in HepaRG human liver cells. Food Chem. Toxicol. 121, 72–81.
Audebert, M., Riu, A., Jacques, C., Hillenweck, A., Jamin, E.L., Zalko, D., Cravedi, J.P., 2010. Use of the γH2AX assay for assessing the genotoxicity of polycyclic aromatic hydrocarbons in human cell lines. Toxicol. Lett. 199, 182–192.
Bodi, D., Ronczka, S., Gottschalk, C., Behr, N., Skibba, A., Wagner, M., These, A., 2014. Determination of pyrrolizidine alkaloids in tea, herbal drugs and honey. Food Addit. Contam. A 31, 1886–1895.
Chen, Z., Huo, J.R., 2010. Hepatic veno-occlusive disease associated with toxicity of pyrrolizidine alkaloids in herbal preparations. Neth. J. Med. 68, 252–260.
Chen, T., Mei, N., Fu, P.P., 2010. Genotoxicity of pyrrolizidine alkaloids. J. Appl. Toxicol. 30, 183–196.
Chen, L., Mulder, P.P.J., Louisse, J., Peijnenburg, A., Wesseling, S., Rietjens, I.M.C.M., 2017. Risk assessment for pyrrolizidine alkaloids detected in (herbal) teas and plant food supplements. Regul. Toxicol. Pharmacol. 86, 292–302.
Chen, L., Ning, J., Louisse, J., Wesseling, S., Rietjens, I.M.C.M., 2018. Use of physiologically based kinetic modelling-facilitated reverse dosimetry to convert in vitro cytotoxicity data to predicted in vivo liver toxicity of lasiocarpine and riddelliine in rat. Food Chem. Toxicol. 116, 216–226.
Chojkier, M., 2003. Hepatic sinusoidal-obstruction syndrome: toxicity of pyrrolizidine alkaloids. J. Hepatol. 39, 437–446.
EFSA, 2016. Dietary exposure assessment to pyrrolizidine alkaloids in the European population. EFSA J 14, 4572.
EFSA CONTAM Panel, 2011. Scientific Opinion on Pyrrolizidine alkaloids in food and feed. EFSA J. 9, 2406.
EFSA CONTAM Panel, 2017. Statement on the risks for human health related to the presence of pyrrolizidine alkaloids in honey, tea, herbal infusions and food supplements. EFSA J. 15, 4908.
EFSA Scientific Committee, 2017. Update: guidance on the use of the benchmark dose approach in risk assessment. EFSA J. 15, 4658.
Frei, H., Lüthy, J., Brauchli, J., Zweifel, U., Würgler, F.E., Schlatte, C., 1992. Structure/activity relationships of the genotoxic potencies of sixteen pyrrolizidine alkaloids assayed for the induction of somatic mutation and recombination in wing cells of Drosophila melanogaster. Chem. Biol. Interact. 83, 1–22.
Fu, P.P., Xia, Q., Lin, G., Chou, M.W., 2004. Pyrrolizidine alkaloids—genotoxicity, metabolism enzymes, metabolic activation, and mechanisms. Drug Metab. Rev. 36, 1–55.
Hartmann, T., Witte, L., 1995. Chemistry, biology and chemoecology of the pyrrolizidine alkaloids. Alkaloids (S. Diego): Chem. Biol. Perspect. 9, 155–233.
Hessel, S., Gottschalk, C., Schumann, D., These, A., Preiss-Weigert, A., Lampen, A., 2014. Structure-activity relationship in the passage of different pyrrolizidine alkaloids through the gastrointestinal barrier: ABCB1 excretes heliotrine and echimidine. Mol. Nutr. Food Res. 58, 995–1004.
Hincks, J.R., Kim, H.Y., Segall, H.J., Molyneux, R.J., Stermitz, F.R., Coulombe Jr., R.A., 1991. DNA cross-linking in mammalian cells by pyrrolizidine alkaloids: structure-activity relationships. Toxicol. Appl. Pharmacol. 111, 90–98.
Hirono, I., Haga, M., Fujii, M., Matsuura, S., Matsubara, N., Nakayama, M., Furuya, T., Hikichi, M., Takanashi, H., Uchida, E., 1979. Induction of hepatic tumors in rats by senkirkine and symphytine. J. Natl. Cancer Inst. 63, 469–472.
Kakar, F., Akbarian, Z., Leslie, T., Mustafa, M.L., Watson, J., van Egmond, H.P., Omar, M.F., Mofleh, J., 2010. An outbreak of hepatic veno-occlusive disease in Western Afghanistan associated with exposure to wheat flour contaminated with pyrrolizidine alkaloids. J. Toxicol. 313280 2010.
Khoury, L., Zalko, D., Audebert, M., 2013. Validation of high-throughput genotoxicity assay screening using γH2AX in-cell western assay on HepG2 cells. Environ. Mol. Mutagen. 54, 737–746.
Kuhara, K., Takanashi, H., Hirono, I., Furuya, T., Asada, Y., 1980. Carcinogenic activity of clivorine, a pyrrolizidine alkaloid isolated from Ligularia dentata. Cancer Lett 10, 117–122.
Kolrep, F., Numata, J., Kneuer, C., Preiss-Weigert, A., Lahrssen-Wiederholt, M., Schrenk, D., These, A., 2018. In vitro biotransformation of pyrrolizidine alkaloids in different species. Part I: microsomal degradation. Arch. Toxicol. 92, 1089–1097.
Liu, X., Klinkhamer, P.G.L., Vrieling, K., 2017. The effect of structurally related metabolites on insect herbivores: a case study on pyrrolizidine alkaloids and western flower thrips. Phytochemistry 138, 93–103.
Lu, C., Zhu, F., Cho, Y.Y., Tang, F., Zykova, T., Ma, W.Y., Bode, A.M., Dong, Z., 2006. Cell apoptosis: requirement of H2AX in DNA ladder formation, but not for the activation of caspase-3. Mol Cell 23, 121–132.
Merz, K.H., Schrenk, D., 2016. Interim relative potency factors for the toxicological risk assessment of pyrrolizidine alkaloids in food and herbal medicines. Toxicol. Lett. 263, 44–57.
Mulder, P.P.J., Sánchez, P.L., These, A., Preiss-Weigert, A., Castellari, M., 2015. Occurrence of pyrrolizidine alkaloids in food. EFSA Support. Publ. 12 (8).
Mulder, P.P.J., López, P., Castellari, M., Bodi, D., Ronczka, S., Preiss-Weigert, A., These, A., 2018. Occurrence of pyrrolizidine alkaloids in animal- and plant-derived food: results of a survey across Europe. Food Addit. Contam. A 35, 118–133.
Nikolova, T., Dvorak, M., Jung, F., Adam, I., Krämer, E., Gerhold-Ay, A., Kaina, B., 2014. The γH2AX assay for genotoxic and nongenotoxic agents: comparison of H2AX phosphorylation with cell death response. Toxicol. Sci. 140, 103–117.
Ning, J., Chen, L., Strikwold, M., Louisse, J., Wesseling, S., Rietjens, I.M.C.M., 2019. Use of an in vitro-in silico testing strategy to predict inter-species and inter-ethnic human differences in liver toxicity of the pyrrolizidine alkaloids lasiocarpine and riddelliine. Arch. Toxicol. 93, 801–818.
Norbury, C.J., Zhivotovsky, B., 2004. DNA damage-induced apoptosis. Oncogene 23, 2797–2808.
NTP, 1978. Bioassay of lasiocarpine for possible carcinogenicity. Natl. Toxicol. Progr. Tech. Rep. 39.
NTP, 2003. Toxicology and carcinogenesis studies of riddelliine (CAS No. 23246-96-0) in F344/N rats and B6C3F1 mice (gavage studies). Natl. Toxicol. Progr. Tech. Rep. 508.
Quesnot, N., Rondel, K., Audebert, M., Martinais, S., Glaise, D., Morel, F., Loyer, P., Robin, M.A., 2016. Evaluation of genotoxicity using automated detection of γH2AX in metabolically competent HepaRG cells. Mutagenesis 31, 43–50.
Robinson, O., Want, E., Coen, M., Kennedy, R., van den Bosch, C., Gebrehawaria, Y., Kudo, H., Sadiq, F., Goldin, R.D., Hauser, M.L., Fenwick, A., Toledano, M.B., Thursz,

M.R., 2014. Hirmi Valley liver disease: a disease associated with exposure to pyrrolizidine alkaloids and DDT. J. Hepatol. 60, 96–102.
Rogakou, E.P., Pilch, D.R., Orr, A.H., Ivanova, V.S., Bonner, W.M., 1998. DNA double-stranded breaks induce histone H2AX phosphorylation on serine 139. J. Biol. Chem. 273, 5858–5868.
Roos, W.P., Kaina, B., 2006. DNA damage-induced cell death by apoptosis. Trends Mol. Med. 12, 440–450.
Ruan, J., Yang, M., Fu, P., Ye, Y., Lin, G., 2014a. Metabolic activation of pyrrolizidine alkaloids: insights into the structural and enzymatic basis. Chem. Res. Toxicol. 27, 1030–1039.
Ruan, J., Liao, C., Ye, Y., Lin, G., 2014b. Lack of metabolic activation and predominant. Formation of an excreted metabolite of nontoxic platynecine-type pyrrolizidine alkaloids. Chem. Res. Toxicol. 27, 7–16.
Shumaker, R., Robertson, K.A., Hsu, I., Allen, J., 1976. Neoplastic transformation in tissues of rats exposed to monocrotaline or dehydroretronecine. J. Natl. Cancer Inst. 56, 787–790.
Wang, J.Y., 2001. DNA damage and apoptosis. Cell Death Differ. 8, 1047–1048.
Wang, Y.P., Yan, J., Fu, P.P., Chou, M.W., 2005. Human liver microsomal reduction of pyrrolizidine alkaloid N-oxides to form the corresponding carcinogenic parent alkaloid. Toxicol. Lett. 155, 411–420.
Wu, X.P., Xiong, M., Xu, C.S., Duan, L.N., Dong, Y.Q., Luo, Y., Niu, T.H., Lu, C.R., 2015. Resveratrol induces apoptosis of human chronic myelogenous leukemia cells in vitro through p38 and JNK-regulated H2AX phosphorylation. Acta Pharmacol. Sin. 36 (3), 353–361.
Yang, M., Ruan, J., Gao, H., Li, N., Ma, J., Xue, J., Ye, Y., Fu, P.P., Wang, J., Lin, G., 2017. First evidence of pyrrolizidine alkaloid N-oxide-induced hepatic sinusoidal obstruction syndrome in humans. Arch. Toxicol. 91, 3913–3925.